Sandbox Results

March 6, 2012

1 The only Flux plot(s)

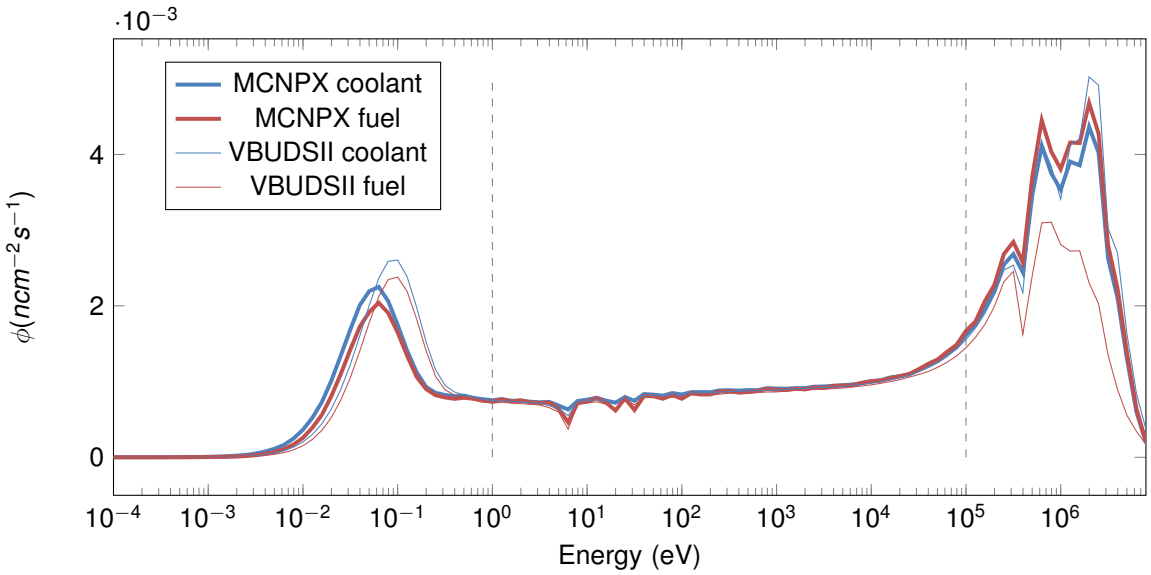

Figure 1: Energy dependent flux in both cells of the reactor, generated by MCNPX and VBUDSII.

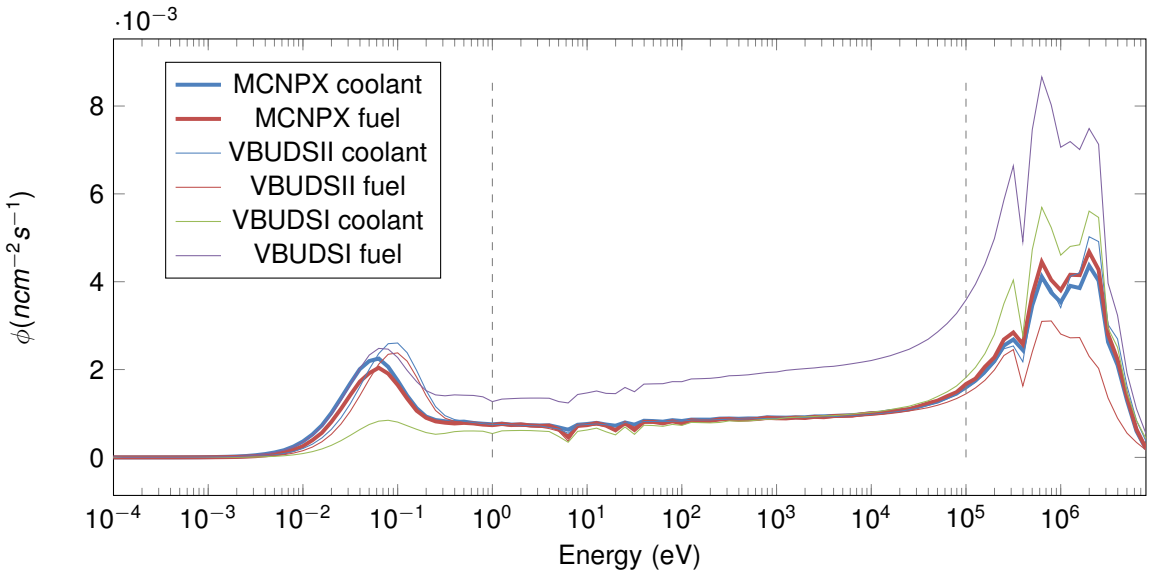

Figure 2: Energy dependent flux in both cells of the reactor, generated by MCNPX, VBUDSII and VBUDSI.

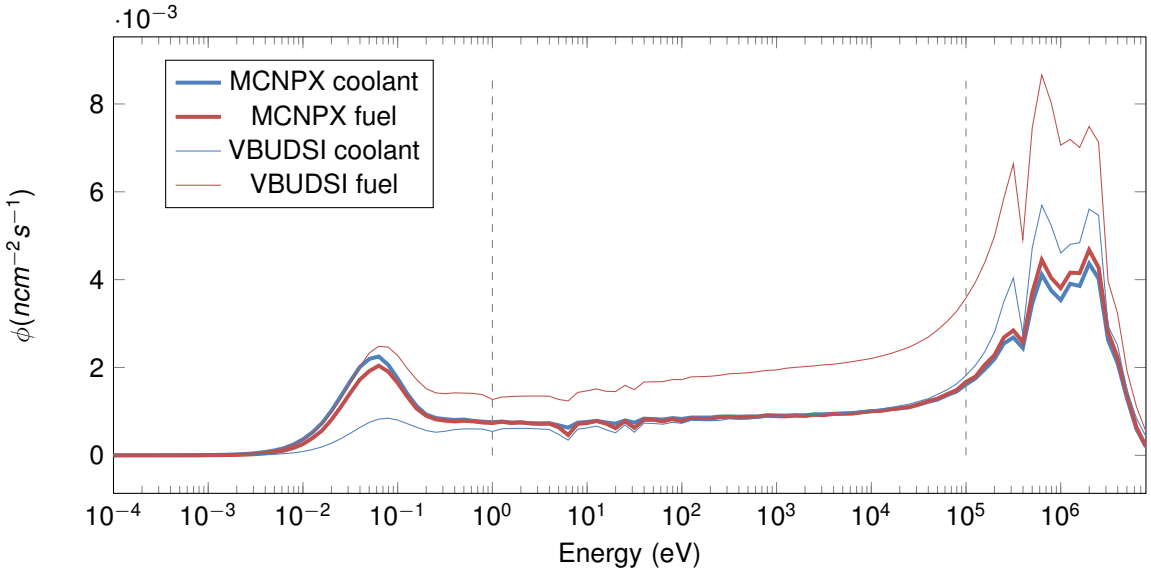

Figure 3: Energy dependent flux in both cells of the reactor, generated by MCNPX and VBUDSI.

1.1 Cross sections in cell H2O

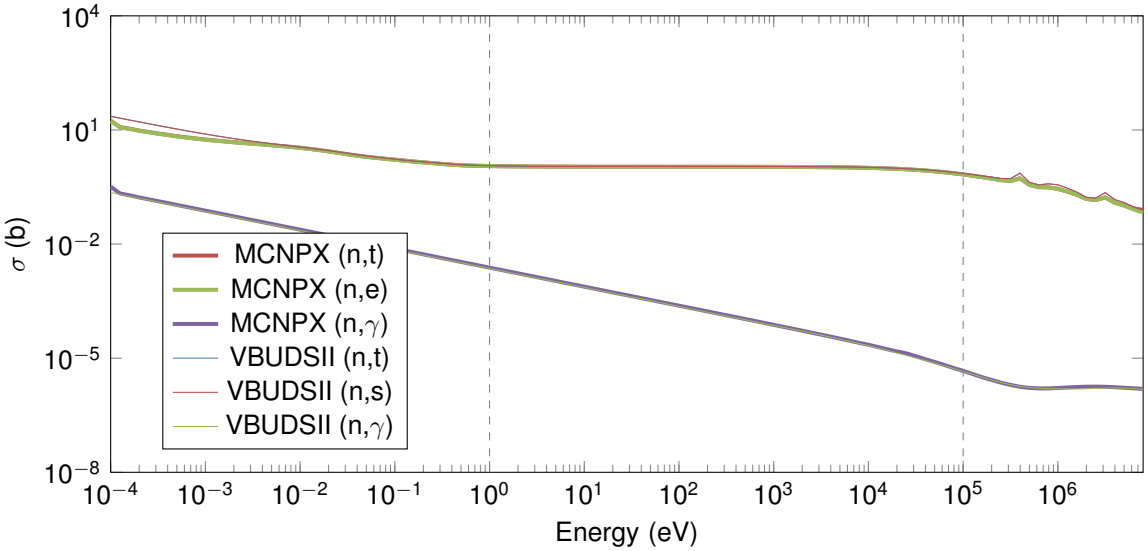

Figure 4: Energy-dependent cross sections for the H2O cell, generated by VBUDSII.

1.1.1 Cross sections in cell H2O, for ZAID 222

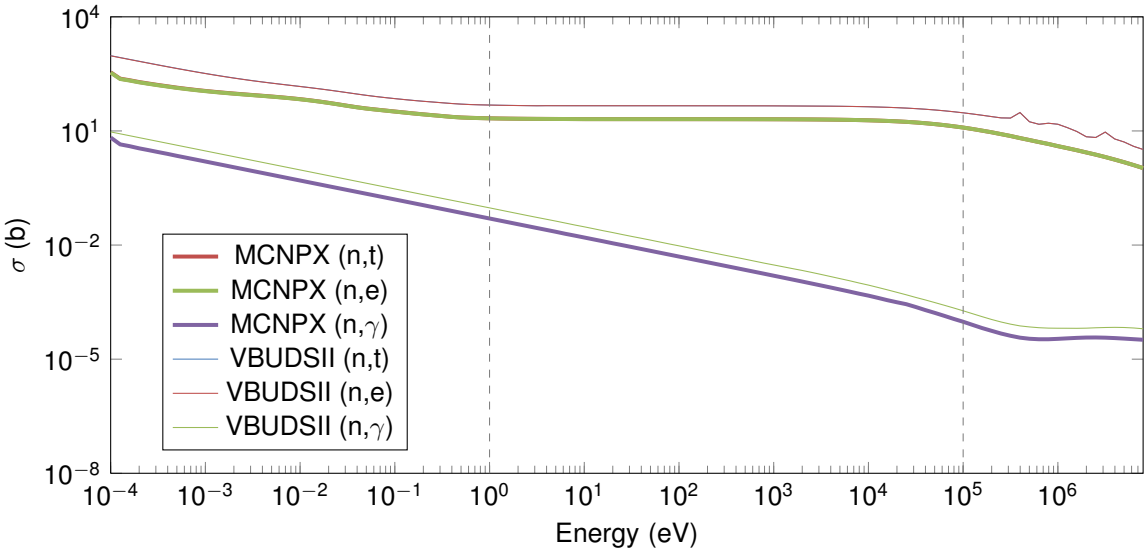

Figure 5: Energy-dependent cross sections in the H2O cell for ZAID 222, generated by both MCNPX and VBUDSII.

1.1.2 Cross sections in cell H2O, for ZAID 222, separated by reaction type

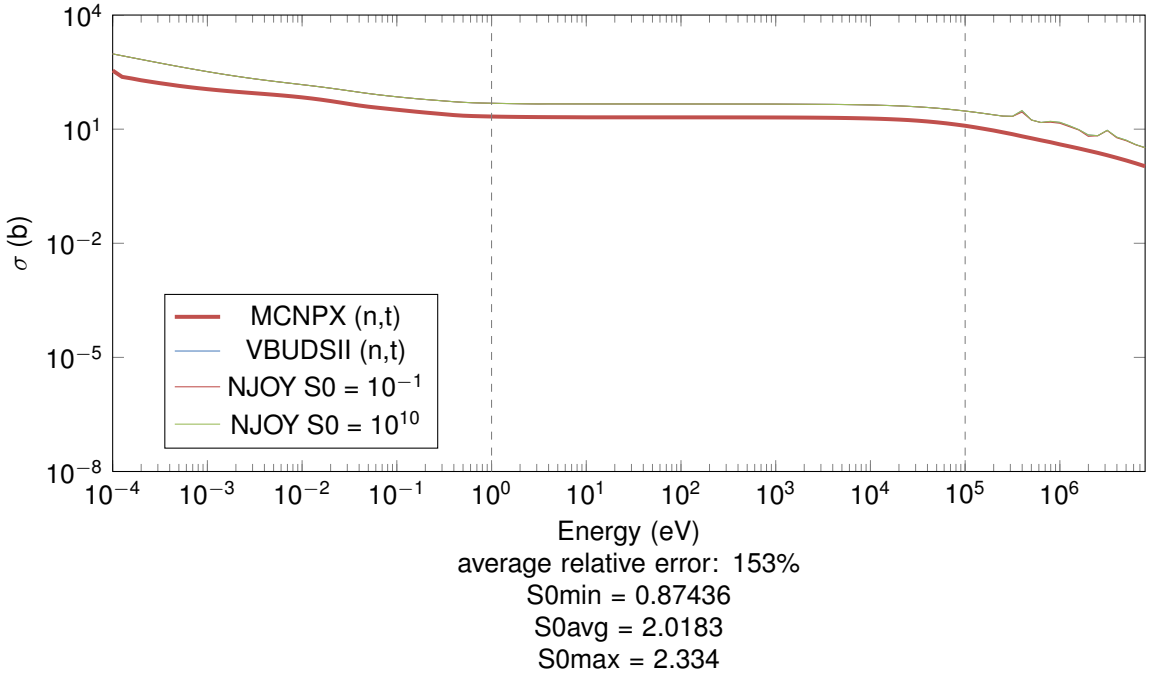

Figure 6: Energy-dependent cross sections in the H2O cell for ZAID 222 and MT 7, generated by both MCNPX and VBUDSII.

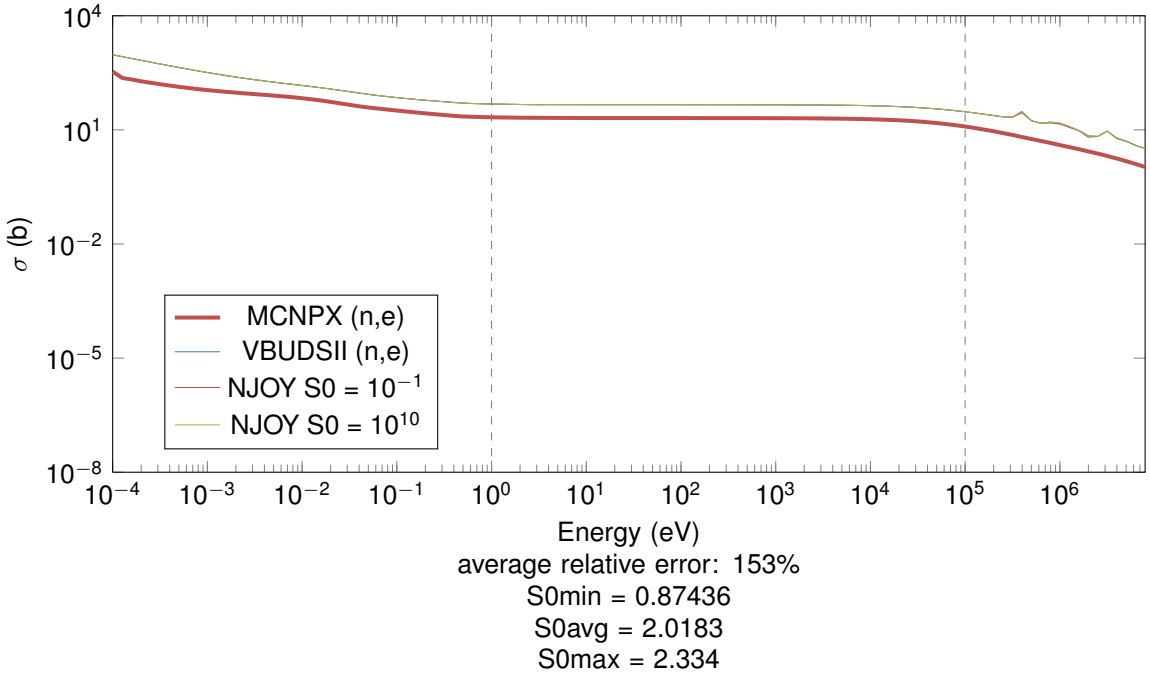

Figure 7: Energy-dependent cross sections in the H2O cell for ZAID 222 and MT 2, generated by both MCNPX and VBUDSII.

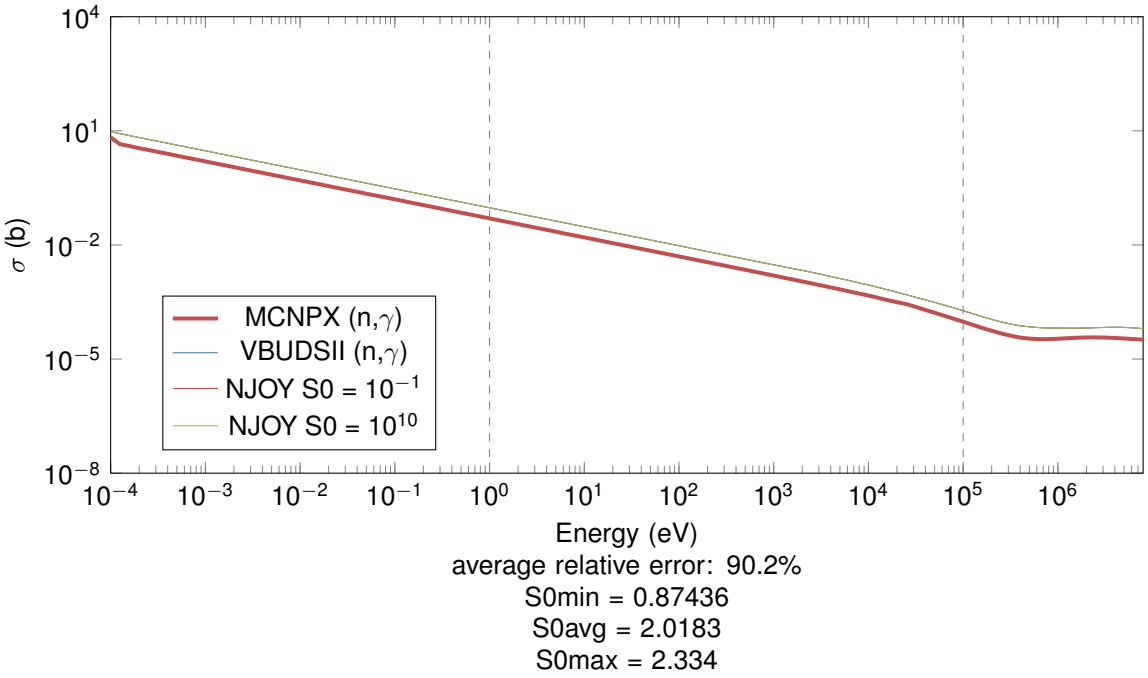

Figure 8: Energy-dependent cross sections in the H2O cell for ZAID 222 and MT 102, generated by both MCNPX and VBUDSII.

1.2 Cross sections in cell UO2

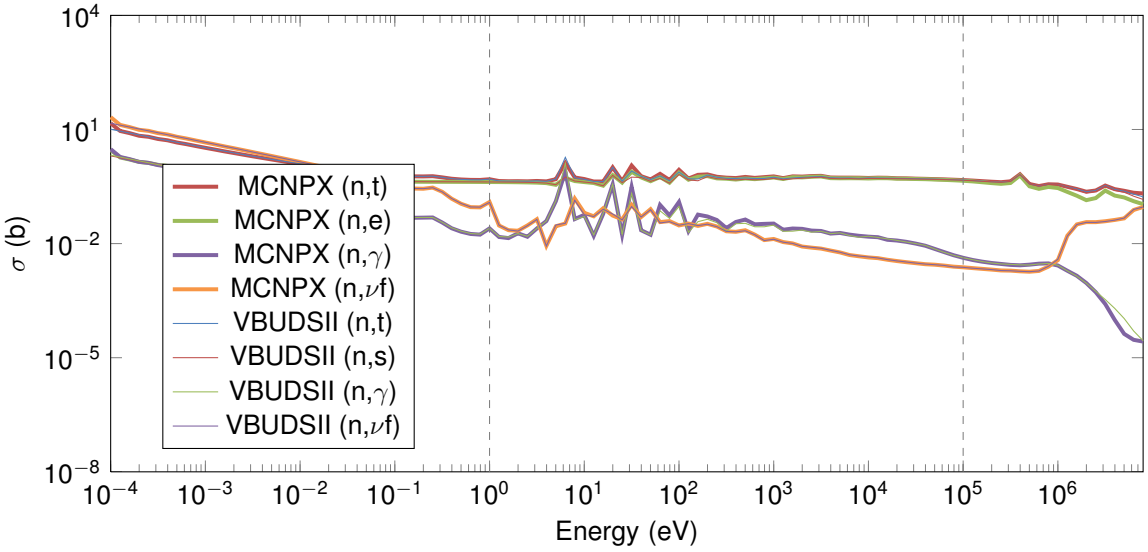

Figure 9: Energy-dependent cross sections for the UO2 cell, generated by VBUDSII.

1.2.1 Cross sections in cell UO2, for ZAID 92235

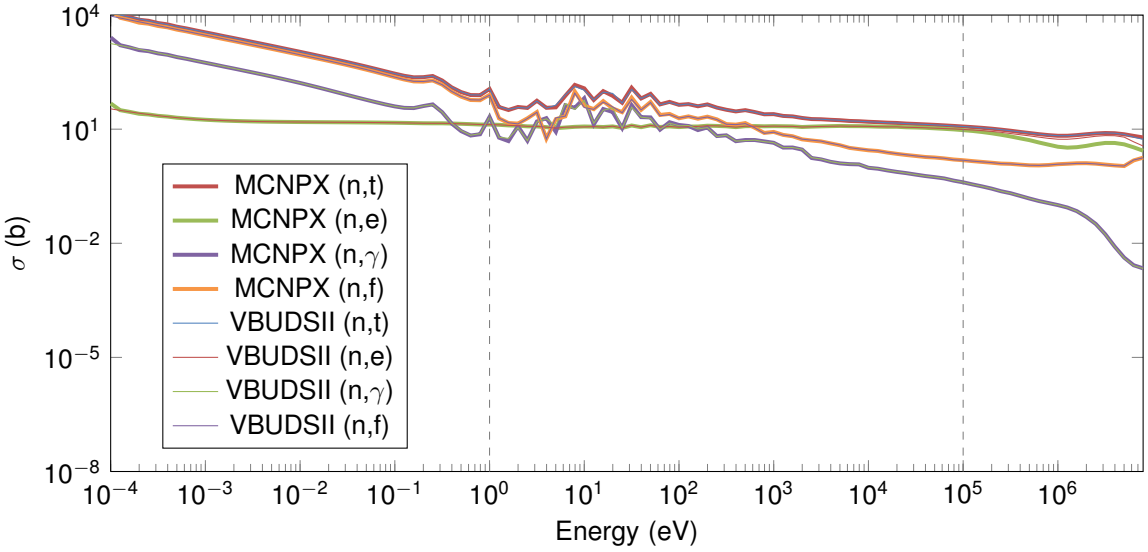

Figure 10: Energy-dependent cross sections in the UO2 cell for ZAID 92235, generated by both MCNPX and VBUDSII.

1.2.2 Cross sections in cell UO2, for ZAID 92235, separated by reaction type

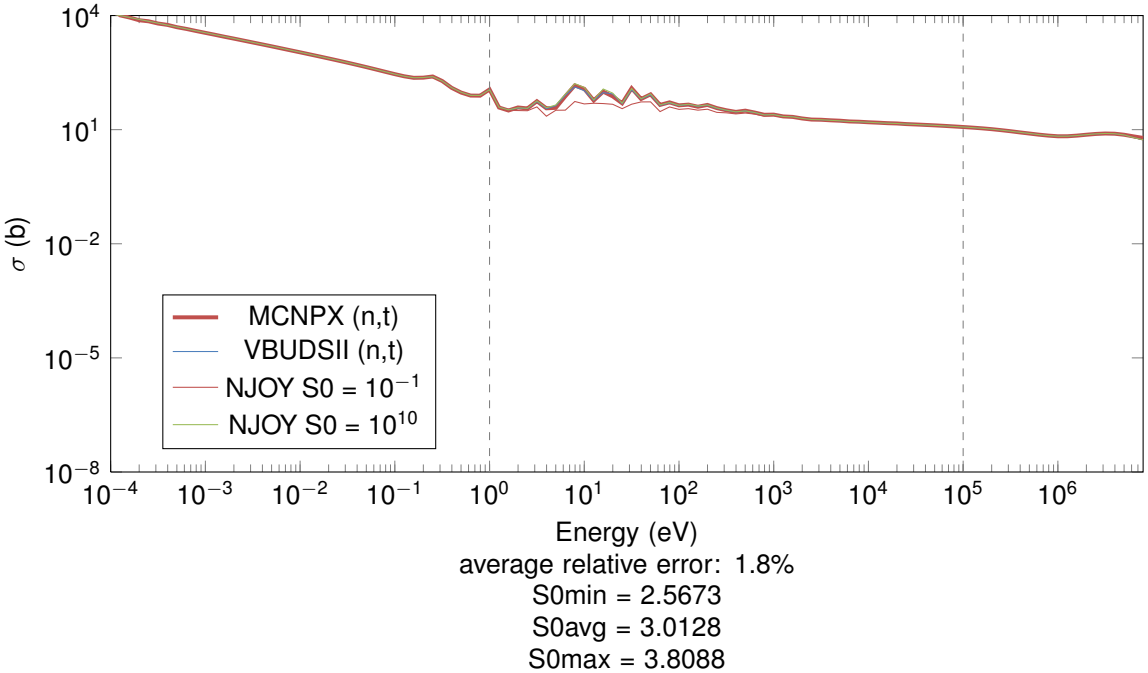

Figure 11: Energy-dependent cross sections in the UO2 cell for ZAID 92235 and MT 7, generated by both MCNPX and VBUDSII.

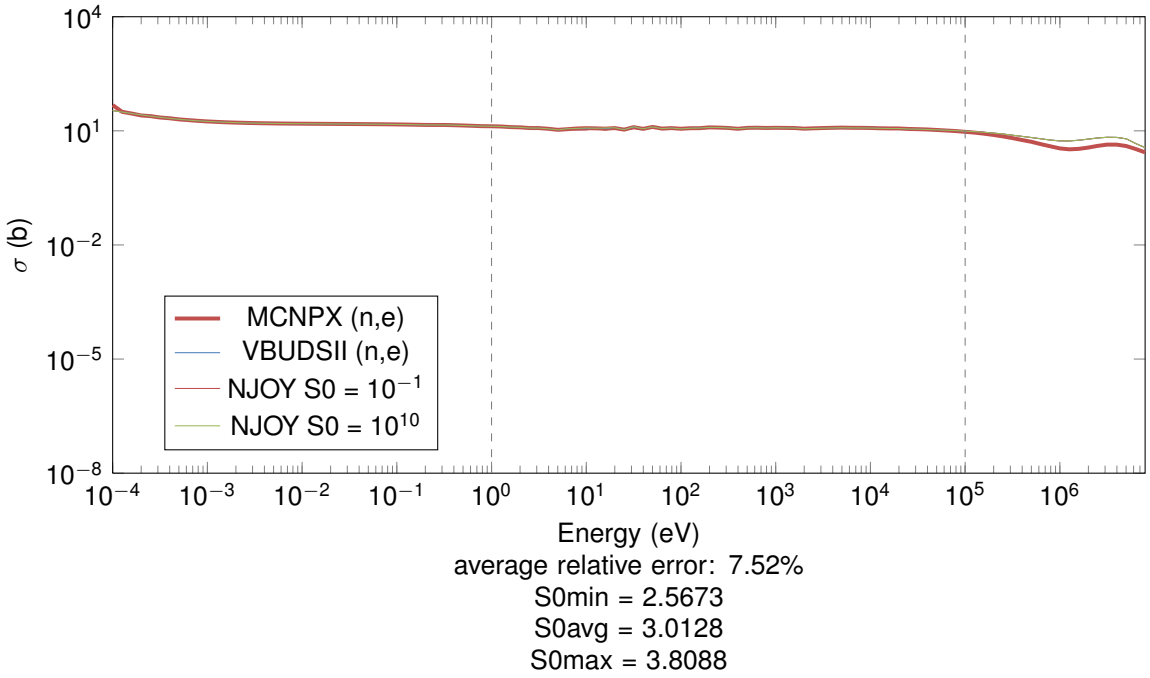

Figure 12: Energy-dependent cross sections in the UO2 cell for ZAID 92235 and MT 2, generated by both MCNPX and VBUDSII.

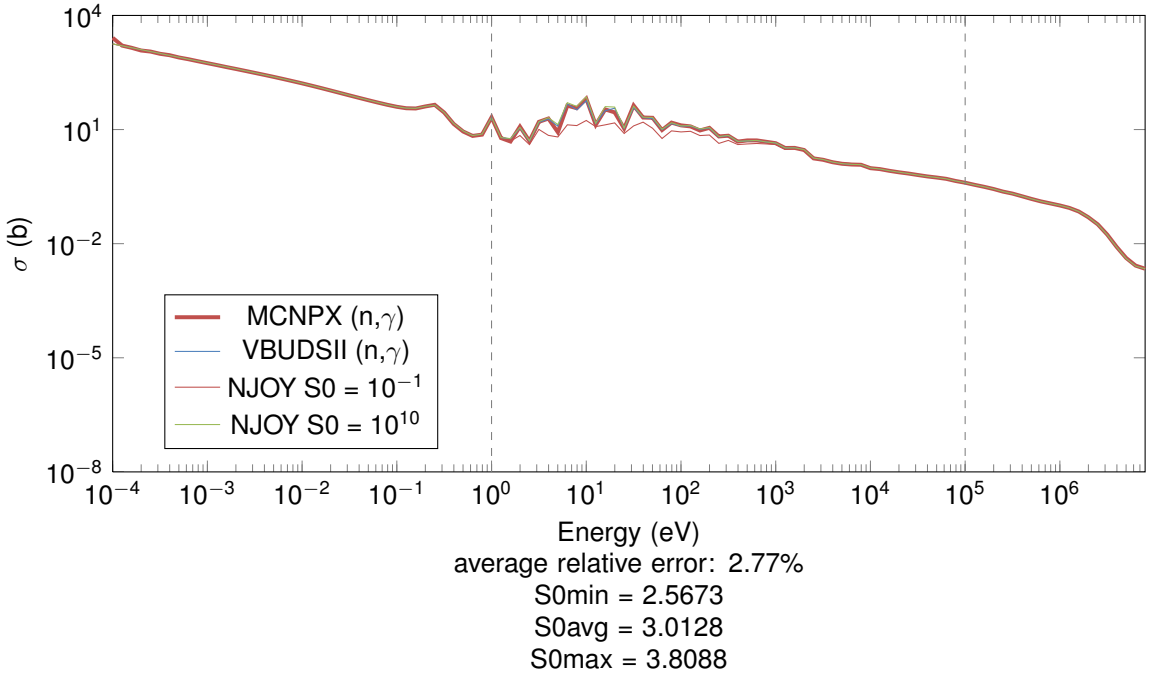

Figure 13: Energy-dependent cross sections in the UO2 cell for ZAID 92235 and MT 102, generated by both MCNPX and VBUDSII.

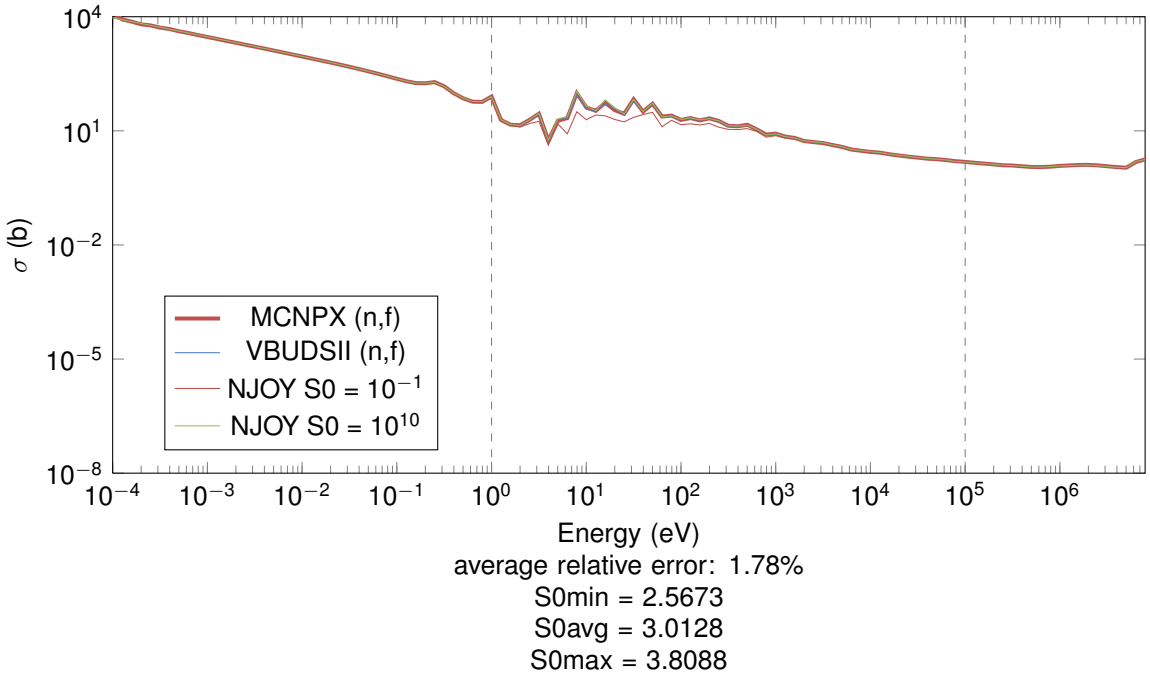

Figure 14: Energy-dependent cross sections in the UO2 cell for ZAID 92235 and MT 18, generated by both MCNPX and VBUDSII.

1.2.3 Cross sections in cell UO2, for ZAID 92238

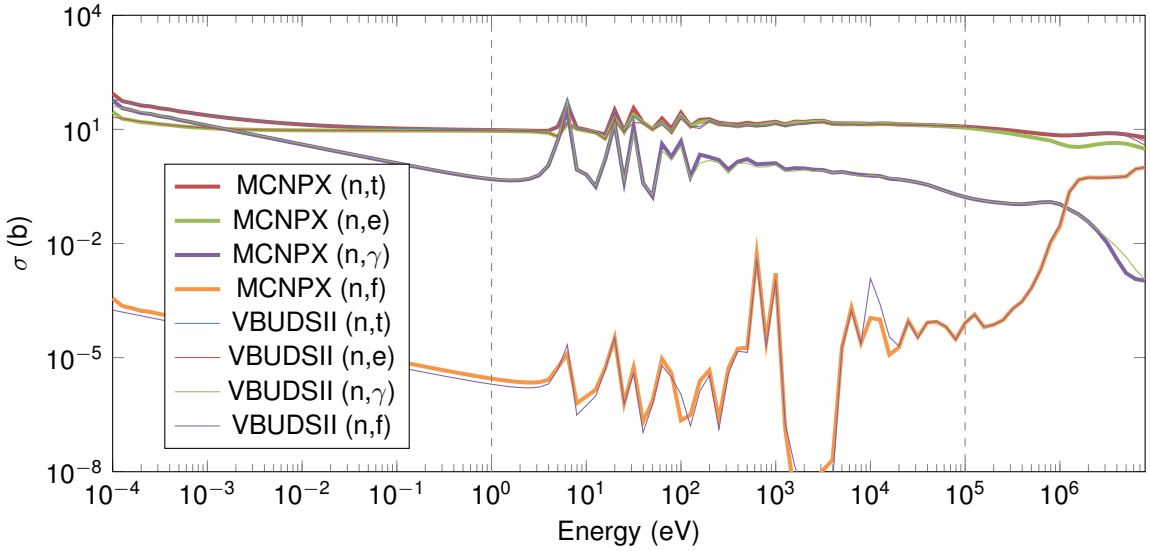

Figure 15: Energy-dependent cross sections in the UO2 cell for ZAID 92238, generated by both MCNPX and VBUDSII.

1.2.4 Cross sections in cell UO2, for ZAID 92238, separated by reaction type

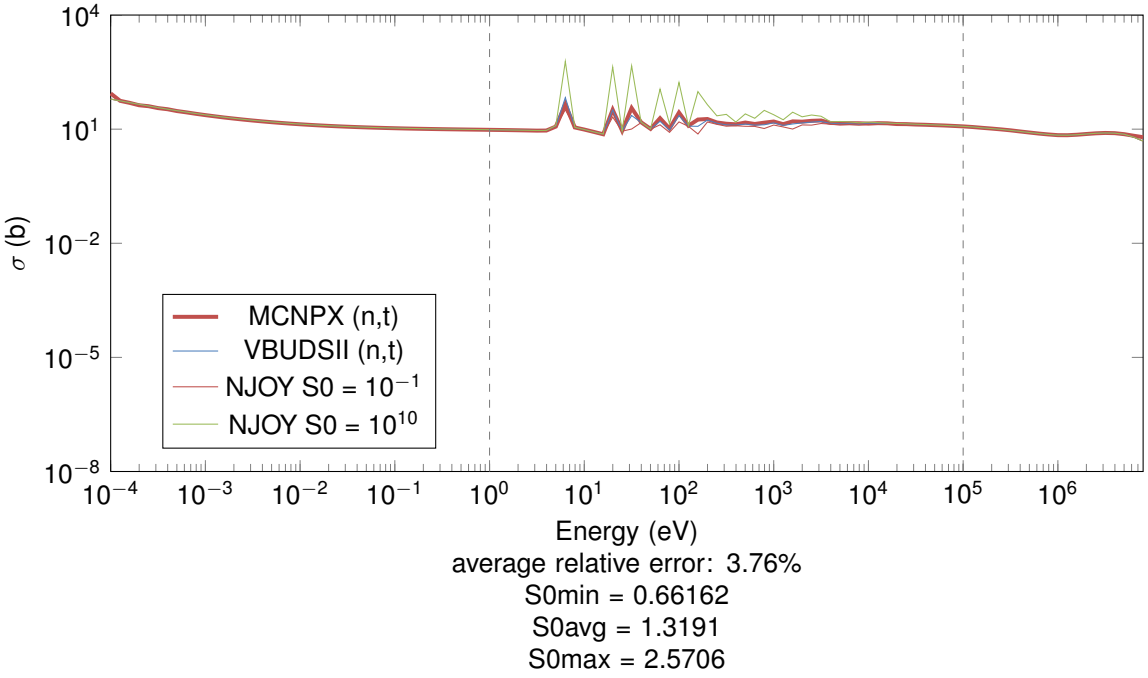

Figure 16: Energy-dependent cross sections in the UO2 cell for ZAID 92238 and MT 7, generated by both MCNPX and VBUDSII.

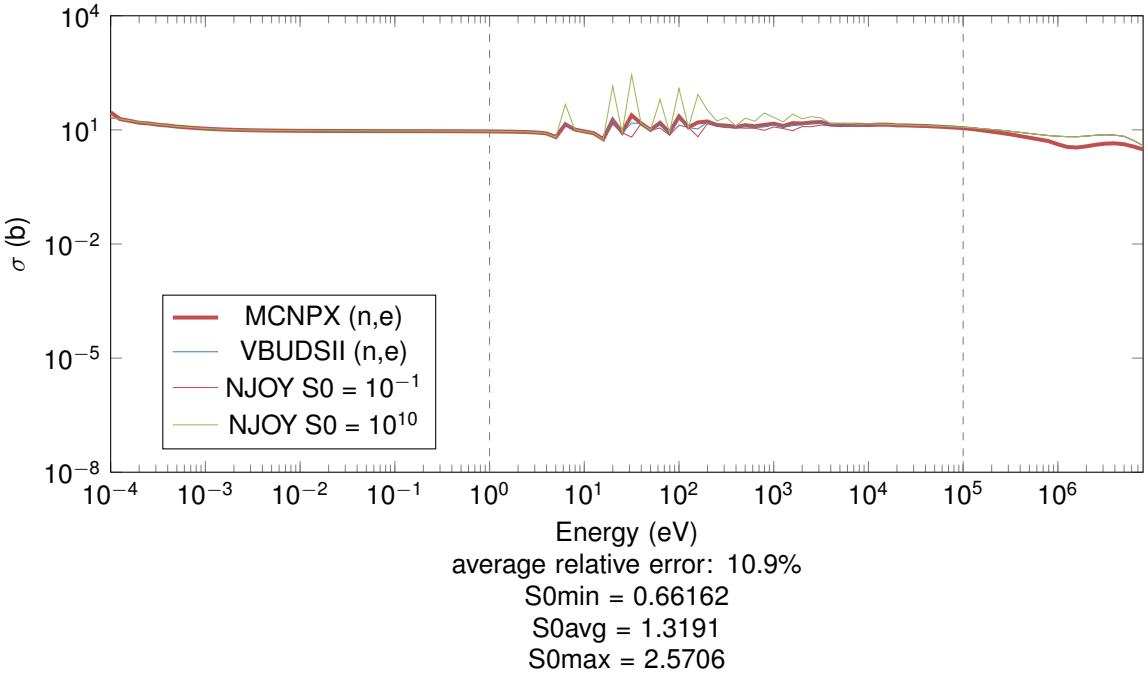

Figure 17: Energy-dependent cross sections in the UO2 cell for ZAID 92238 and MT 2, generated by both MCNPX and VBUDSII.

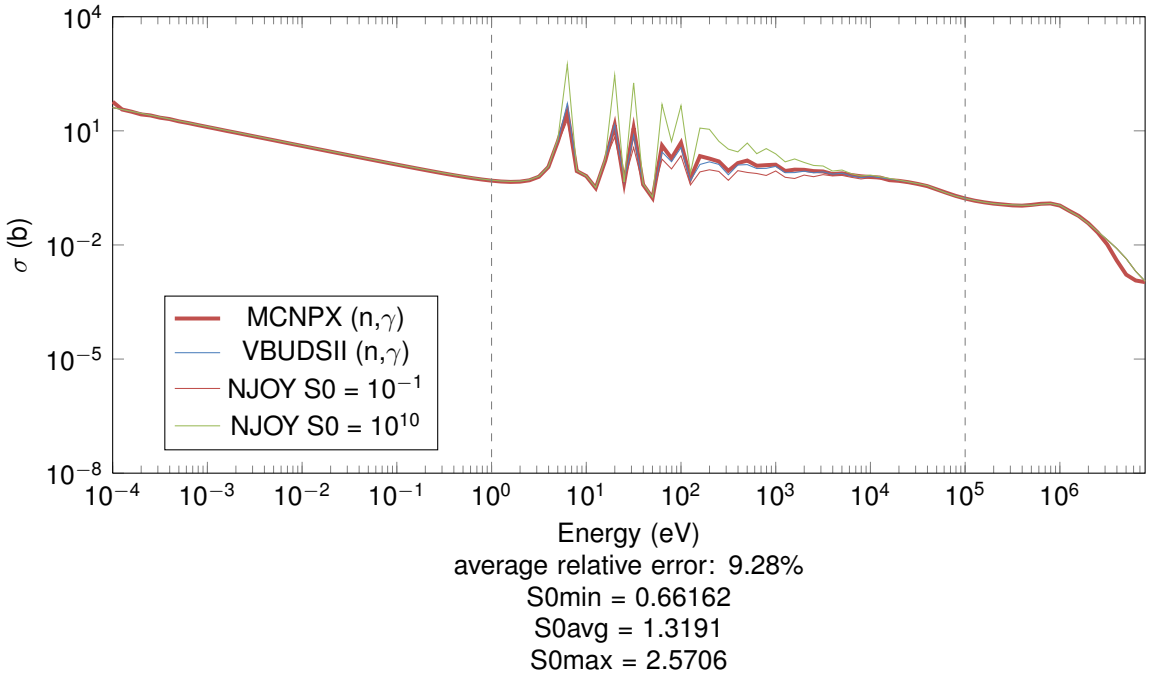

Figure 18: Energy-dependent cross sections in the UO2 cell for ZAID 92238 and MT 102, generated by both MCNPX and VBUDSII.

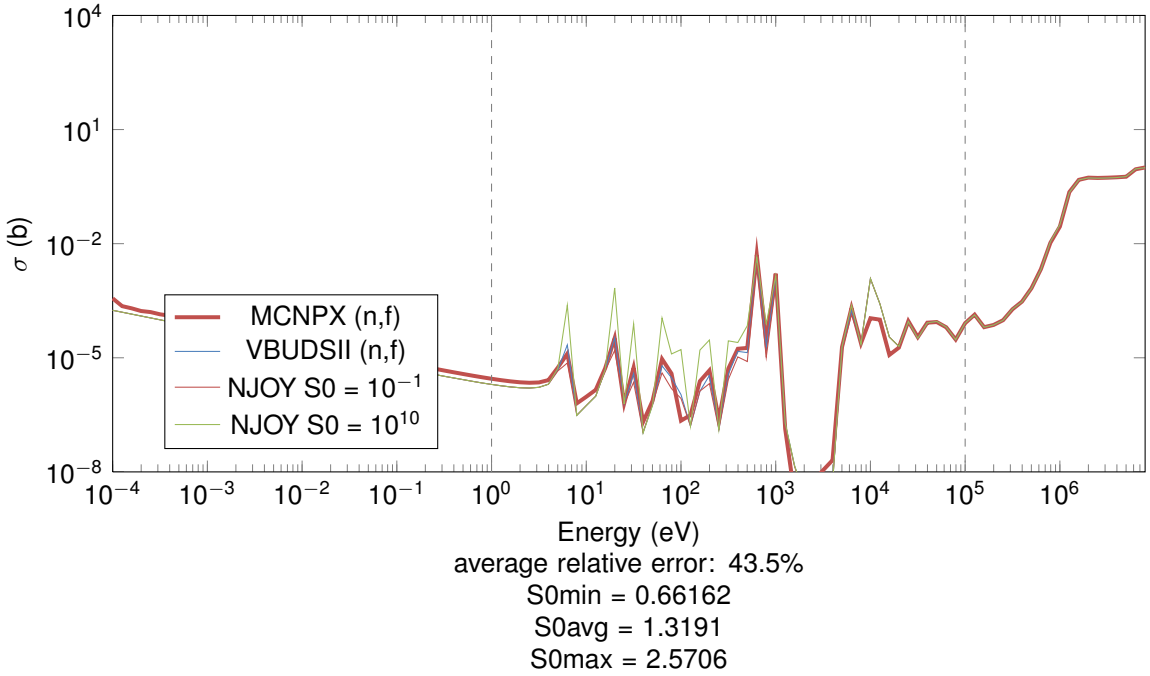

Figure 19: Energy-dependent cross sections in the UO2 cell for ZAID 92238 and MT 18, generated by both MCNPX and VBUDSII.

1.2.5 Cross sections in cell UO2, for ZAID 8016

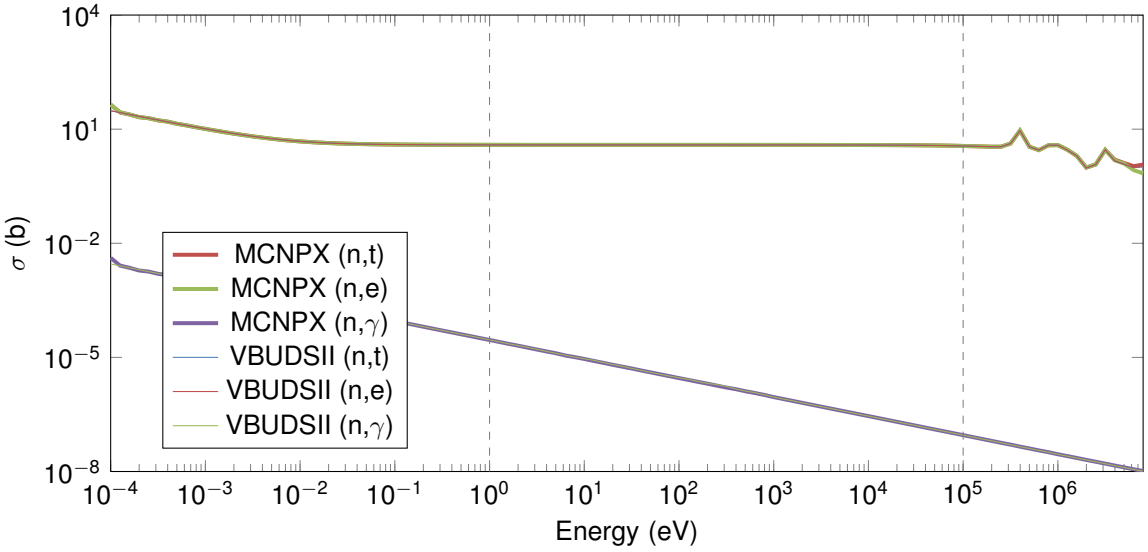

Figure 20: Energy-dependent cross sections in the UO2 cell for ZAID 8016, generated by both MCNPX and VBUDSII.

1.2.6 Cross sections in cell UO2, for ZAID 8016, separated by reaction type

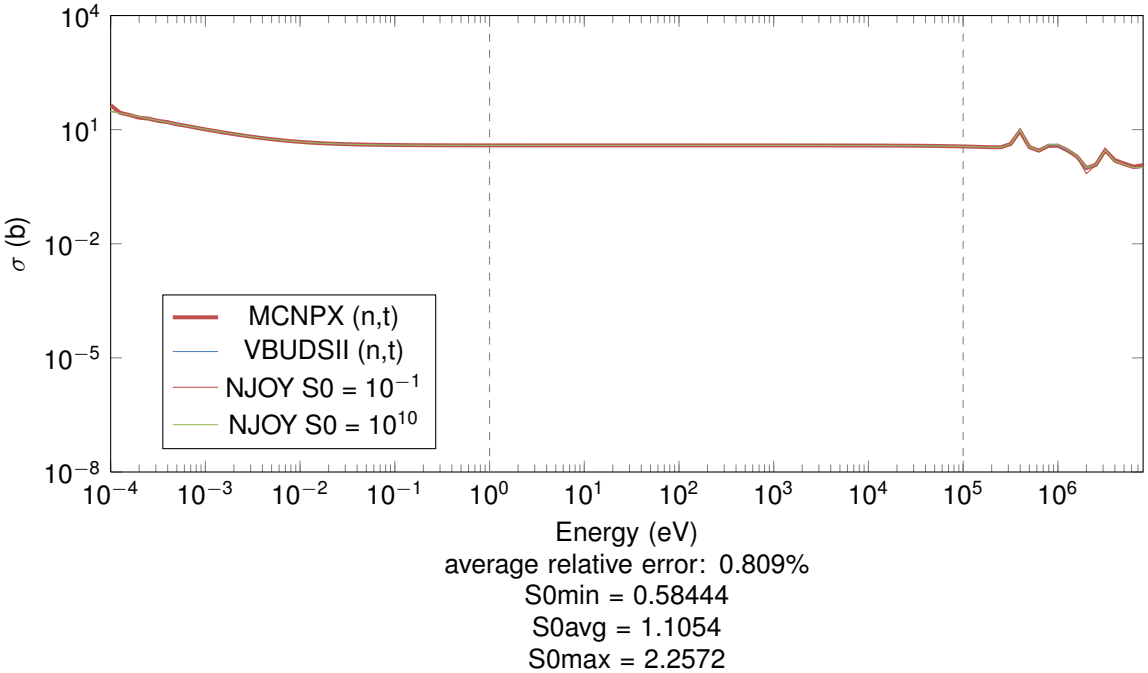

Figure 21: Energy-dependent cross sections in the UO2 cell for ZAID 8016 and MT 7, generated by both MCNPX and VBUDSII.

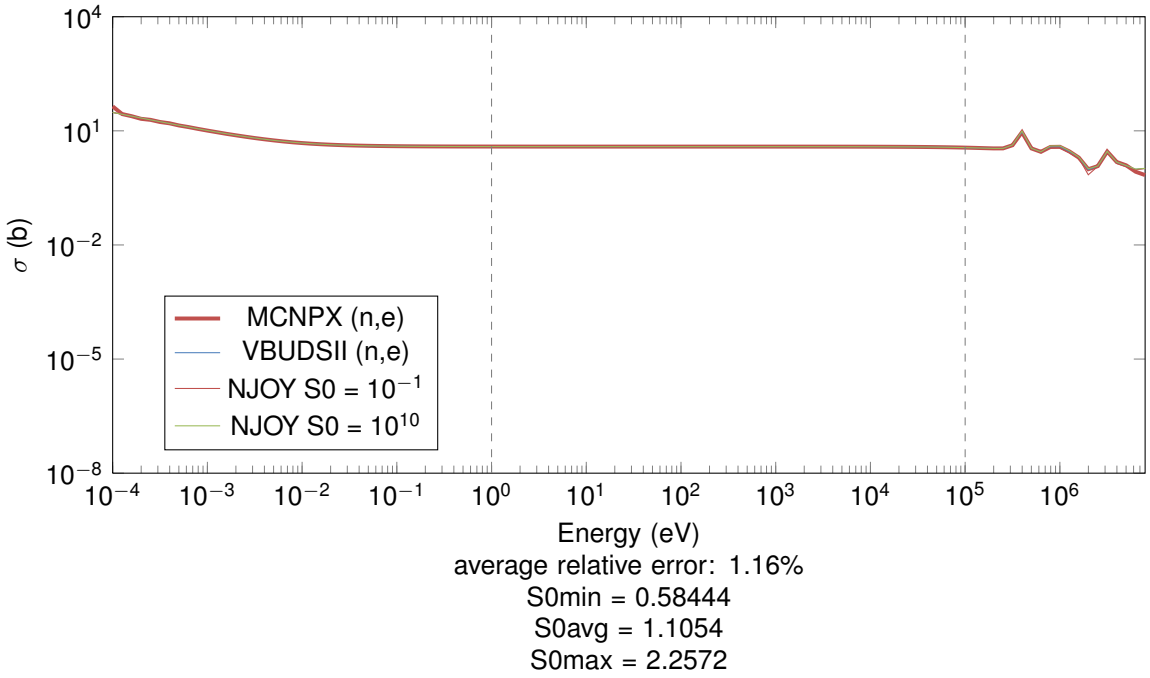

Figure 22: Energy-dependent cross sections in the UO2 cell for ZAID 8016 and MT 2, generated by both MCNPX and VBUDSII.

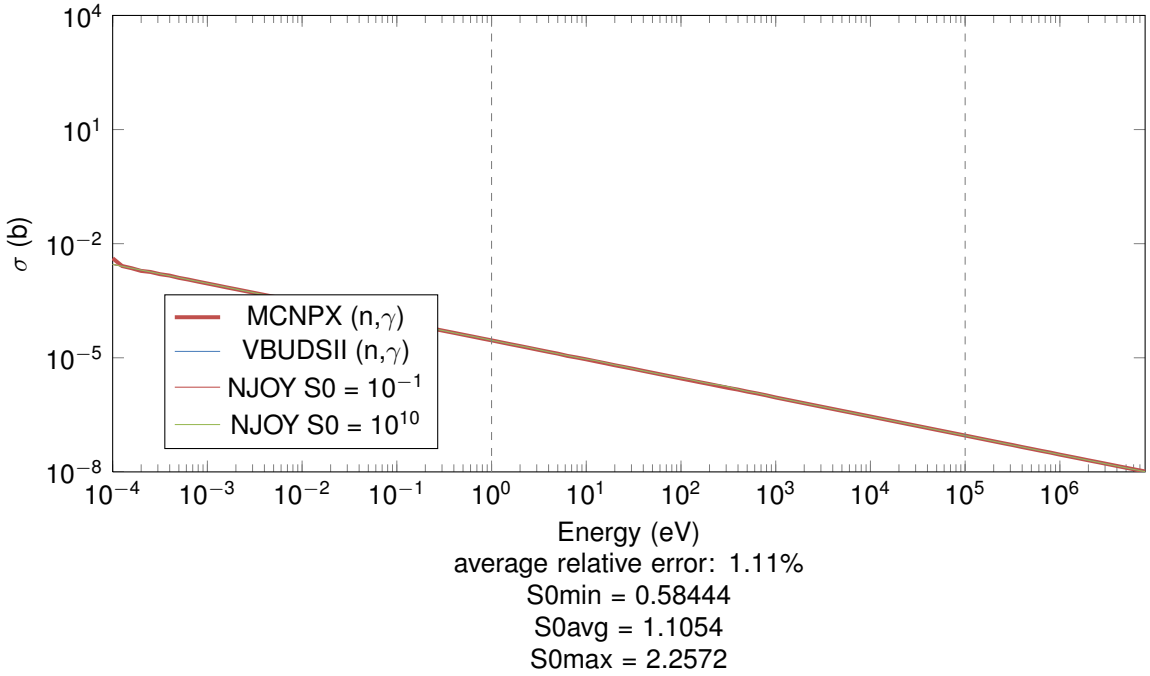

Figure 23: Energy-dependent cross sections in the UO2 cell for ZAID 8016 and MT 102, generated by both MCNPX and VBUDSII.

MT 7: total

MT 4: inelastic scattering
MT 2: elastic scattering
MT 102: radiative capture
MT 18: fission
XS error 1: `nanmean(abs(V-M)./M)`
XS error 2: `V'*M/norm(V)/norm(M)`
XS error 3: `log10(V)'*log10(M)/norm(log10(V))/norm(log10(M))`

cell	ZAID	MT	XS error 1	XS error 2	XS error 3	VBUDSII RR	MCNPX RR	RR error
1	222	7	1.53	NaN	NaN	4.8	2.09	1.29
1	222	2	1.53	NaN	NaN	4.79	2.09	1.3
1	222	102	0.9	NaN	NaN	$9.91 \cdot 10^{-3}$	$5.73 \cdot 10^{-3}$	0.73
2	92,235	7	$1.8 \cdot 10^{-2}$	NaN	NaN	10.27	11.1	$7.45 \cdot 10^{-2}$
2	92,235	2	$7.52 \cdot 10^{-2}$	NaN	NaN	1.1	1.12	$1.51 \cdot 10^{-2}$
2	92,235	102	$2.77 \cdot 10^{-2}$	NaN	NaN	1.58	1.68	$6.04 \cdot 10^{-2}$
2	92,235	18	$1.78 \cdot 10^{-2}$	NaN	NaN	7.6	8.21	$7.42 \cdot 10^{-2}$
2	92,238	7	$3.76 \cdot 10^{-2}$	NaN	NaN	1.15	1.34	0.14
2	92,238	2	0.11	NaN	NaN	1.04	1.08	$4 \cdot 10^{-2}$
2	92,238	102	$9.28 \cdot 10^{-2}$	NaN	NaN	0.11	0.11	$4.75 \cdot 10^{-2}$
2	92,238	18	0.44	NaN	NaN	$6.35 \cdot 10^{-3}$	$1.23 \cdot 10^{-2}$	0.48
2	8,016	7	$8.09 \cdot 10^{-3}$	NaN	NaN	0.38	0.43	0.12
2	8,016	2	$1.16 \cdot 10^{-2}$	NaN	NaN	0.38	0.43	0.12
2	8,016	102	$1.11 \cdot 10^{-2}$	NaN	NaN	$2.64 \cdot 10^{-6}$	$2.78 \cdot 10^{-6}$	$4.93 \cdot 10^{-2}$